Computer mechanization of six-degree of freedom flight equations

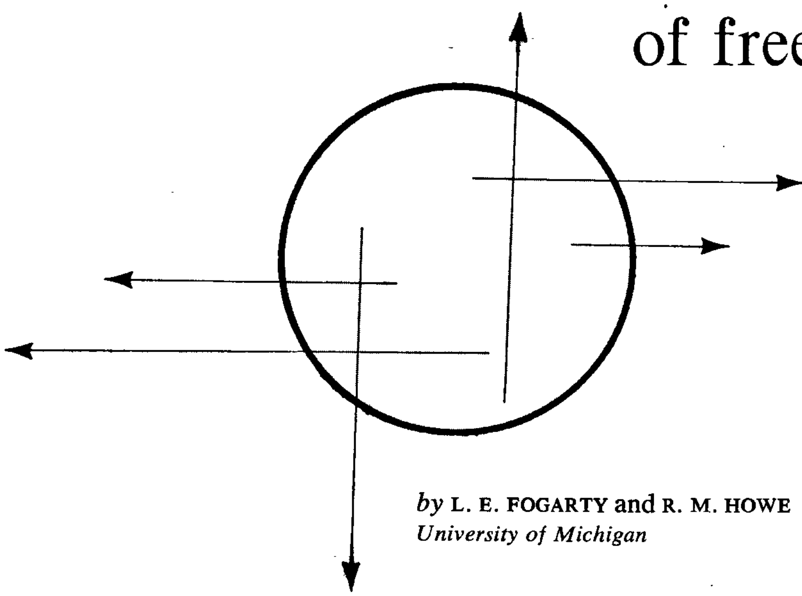

by L. E. FOGARTY and R. M. HOWE
University of Michigan

The authors were introduced last month when we published their article *Trajectory optimization by a direct descent process.*

Preparation of this paper was supported under NASA contract NASr 54(06).

1. INTRODUCTION

Solution of the six-degree-of-freedom flight equations for aircraft and missiles continues to represent one of the most important application areas for analog, hybrid, and digital computer systems. Important computer requirements such as accuracy and speed are very much dependent on the choice of axis system for the translation equations of motion. In this connection it is well known that the flight-path axis system makes much lower accuracy and speed demands on the computer than does the body-axis system.[1,2] Despite this, a number of current computer mechanizations continue to use body axes for solving the translational equations of motion. Because of this, unnecessary demands on accuracy or frequency response are placed on the computer, and many mechanizations which could be all-analog or all-digital have shifted to hybrid implementation. Even if the mechanization is hybrid from the outset, there is considerable advantage to be gained by using an efficient axis system. The purpose of this paper is to point out again the advantages of flight path axes and to summarize the overall equation requirements for solving the six-degree of freedom flight equations.

2. BODY-AXIS TRANSLATIONAL EQUATIONS

For comparison, we present first the body-axis translational equations. The body axes x_b, y_b, and z_b are defined as a right-hand set fixed to the vehicle with the x_b axis along the longitudinal axis and the z_b axis directed downward for normal level flight. The components of the total vehicle velocity vector $\vec{V}_p$ along the x_b, y_b, and z_b axes, respectively, are U_b, V_b, and W_b (see figure 2.1).

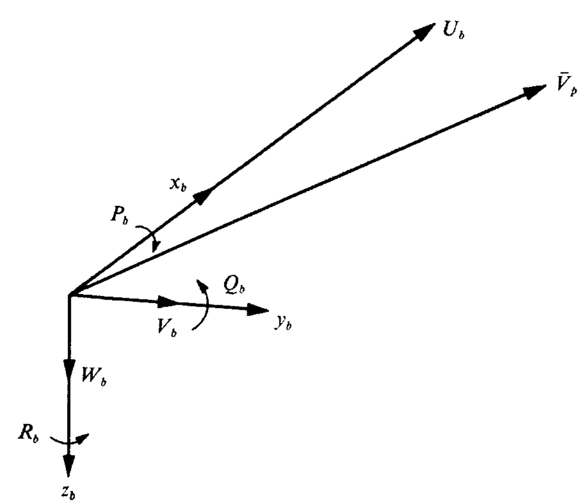

Figure 2.1—Body axes x_b, y_b, z_b with velocity components U_b, V_b, and W_b and angular velocity components P_b, Q_b, and R_b, respectively

The components of the body-axis angular velocity vector $\vec{\Omega}$ (and hence the vehicle angular velocity vector) along the x_b, y_b, and z_b axes are P_b, Q_b, and R_b, *i.e.*, roll rate, pitch rate, and yaw rate, respectively. Here we assume $\vec{V}_p$ and $\vec{\Omega}$ represent vehicle translational and rotational velocity vectors as viewed from an inertial (nonaccelerating) frame of reference. If we denote the external forces along a set of coordinate axes by X, Y, and Z, respectively, then Euler's translational equations of motion, which are obtained by summing forces along the coordinate axes, are the following:

$$m(\dot{U} - VR + WQ) = X \tag{2.1}$$

$$m(\dot{V} - WP + UR) = Y \tag{2.2}$$

$$m(\dot{W} - UQ + VP) = Z \tag{2.3}$$

where m is the mass of the vehicle.

The inefficiency of these equations in body axes is immediately apparent when one considers the approximate size of the various terms. Let the vehicle be, say, a Mach 2 aircraft with $V_{max} = 2000$ feet per second. A reasonable upper limit on pitch-rate Q_b might be 2 radians per second. Thus, the term U_bQ_b in equation (2.3) might be as large as 4000 ft/s^2 or 125 g's. On the other hand Z_b/m, the normal acceleration due to the external force (primarily gravity and aerodynamic lift) may have an upper limit of several g's. Hence artificial accelerations which are perhaps 20 to 50 times greater than the actual accelerations are introduced because of the high rotation rates which the body-axes experience. This means much less favorable computer scaling and hence much poorer solution accuracy for a given computer precision. Furthermore, the high-speed dynamics of the rotational equations are coupled into the translational equations, thus placing severe dynamic response requirements on the computer.

The use of flight-path axes greatly alleviates these problems. As we shall see in the next section, the flight-path axes allow a more efficient calculation of the aerodynamic angle of attack α and the aerodynamic angle of sideslip β than body axes allow. Using body axes and assuming that the ambient air mass is not moving relative to the inertial frame used to define $\vec{V}_p$, then the following formulas can be used to obtain α, β, and velocity magnitude V_p from the body-axis velocity components U_b, V_b, and W_b:

$$\tan \alpha = \frac{W_b}{U_b} \tag{2.4}$$

$$\sin \beta = \frac{V_b}{V_p} \tag{2.5}$$

$$V_p = \frac{U_b}{\cos \alpha \cos \beta} = (U_b^2 + V_b^2 + W_b^2)^{1/2}. \tag{2.6}$$

3. FLIGHT-PATH AXIS TRANSLATIONAL EQUATIONS

Next consider the flight-path axes x_w, y_w, z_w shown in figure 3.1. These differ from the body axes x_b, y_b, z_b by the angle of attack α and the angle of sideslip β, as shown in the figure. To rotate from body axes to flight-path axes one first pitches the body axes about y_b through $-\alpha$. This defines an intermediate axis system x_s, y_s z_s, called stability axes. One then yaws about z_s, through β, which defines the flight-path axes x_w, y_w, and z_w. Note that V_p is the x_w component of vehicle velocity; the y_w and z_w components are zero by definition. Let us define the x_w, y_w, and z_w components of flight-path angular velocity relative to inertial space by P_w, Q_w, and R_w, and the components of external force along x_w, y_w, and z_w by X_w, Y_w, and Z_w, respectively. Then, since $U_w \equiv V_p$ and $V_w = W_w \equiv 0$, the translational equations (2.1), (2.2), and (2.3) referred to the flight-path axes become

$$m\dot{V}_p = X_w \tag{3.1}$$

$$mV_pR_w = Y_w \tag{3.2}$$

$$-mV_pQ_w = Z_w \tag{3.3}$$

Solution of these three equations results in total velocity V_p, flight-path axis yaw rate R_w, and flight-path axis pitch rate Q_w.

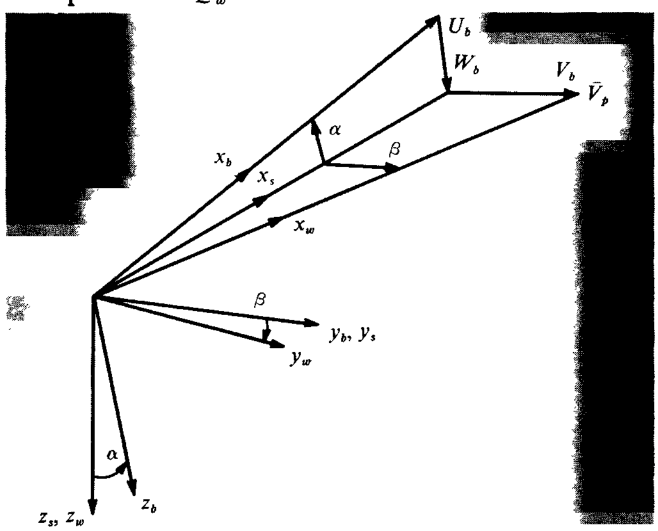

Figure 3.1—Flight path axes x_w, y_w, z_w and the relation to body axes x_b, y_b, z_b

Next consider the formulas for α and β. Reference to figure 3.1 shows that $\dot{\alpha}$ is directed along y_s with a component $\dot{\alpha} \cos \beta$ along y_w. Thus $\dot{\alpha} \cos \beta$ is equal to the difference between body-axis and flight-path axis angular rates along y_w. Therefore, from equation (3.3) we can write

$$\dot{\alpha} \cos \beta = Q_b \cos \beta - P_b^s \sin \beta + \frac{Z_w}{mV_p} \tag{3.4}$$

where P_b^s is the body-axis (not stability axis) angular rate along x_s and is given by

$$P_b^s = P_b \cos\alpha + R_b \sin\alpha \qquad (3.5)$$

Similarly, reference to figure 3.1 shows that $\dot{\beta}$ is directed along z_w and is equal to the difference between flight-path axis and body axis angular rates along z_w. Thus from equation (3.2)

$$\dot{\beta} = \frac{Y_w}{mV_p} - R_b^s \qquad (3.6)$$

where R_b^s is the body-axis angular rate along z_s and is given by

$$R_b^s = -P_b \sin\alpha + R_b \cos\alpha \qquad (3.7)$$

(Note that

$$Q_b^s = Q_b \qquad (3.8)$$

since the y_b body axis and y_s stability axis are coincident.)

Equations (3.1), (3.4), and (3.6) can be integrated to yield total velocity V_p, angle of attack α, and angle of sideslip β. They do not present the scaling difficulty of equations (2.1), (2.2), and (2.3) in the body axes. The body-axis velocity components U_b, V_b, and W_b can be obtained from V_p, α, and β by the formulas

$$U_b = V_p \cos\alpha \cos\beta \qquad (3.9)$$

$$V_b = V_p \sin\beta \qquad (3.10)$$

$$W_b = V_p \sin\alpha \cos\beta \qquad (3.11)$$

Similarly, the flight-path-axis forces X_w, Y_w, and Z_w can be derived from body-axis force components X_b, Y_b, and Z_b by the formulas

$$\left.\begin{aligned} X_s &= X_b \cos\alpha + Z_b \sin\alpha \\ X_w &= X_s \cos\beta + Y_s \sin\beta \end{aligned}\right\} \qquad (3.12)$$

$$Y_s = Y_b, \qquad Y_w = -X_s \sin\beta + Y_s \cos\beta \qquad (3.13)$$

$$Z_s = -X_b \sin\alpha + Z_b \cos\alpha, \qquad Z_w = Z_s \qquad (3.14)$$

where X_s, Y_s, and Z_s are the intermediate stability-axis force components.

Frequently the aerodynamic force components are computed along stability axes, in which case the power plant and gravity forces, computed in body axes, would be resolved into stability axes where the aerodynamic forces are added; then the total forces would be resolved into flight-path axes to allow use of equations (3.1), (3.4), and (3.6).

It should be noted that we have assumed throughout this section that the translational and rotational velocity vectors are velocities relative to an inertial reference frame. If the atmosphere through which the vehicle is flying can be considered to be fixed with respect to this inertial frame, then the velocity magnitude V_p is the vehicle velocity relative to the atmosphere, and α and β represent the aerodynamic angle of attack and sideslip, respectively. Using the approximation that the earth is flat, and with constant surface winds, it is possible to define the inertial reference frame as a frame attached to the atmosphere. Then all the formulas, as presented, are correct, and α, β and V_p can be used for computation of aerodynamic forces and moments.

Unfortunately, for a rotating spherical earth, axes fixed in the atmosphere are not inertial. If we consider such a frame to be inertial, we will make acceleration errors in equations (3.1), (3.2), and (3.3) of the order of $\hat{V}^2/r_0$ where $\hat{V}$ is the vehicle velocity relative to an inertial frame with origin at the center of the earth and r_0 is the radius of the earth. For illustration, consider a vehicle flying eastward in still air with a velocity V_a relative to the atmosphere. Then $\hat{V} \cong V_a + r_0\omega_N \cos L$, where ω_N is the earth spin rate and L is the latitude. If the vehicle is flying westward, $\hat{V} \cong V_a - r_0\omega_N \cos L$. For other headings $\hat{V}$ lies between these values.

For example, if $V_a = 3000$ ft/s and $L = 0$ degrees, $\hat{V}$ ranges between approximately 1600 and 4400 ft/s. The corresponding acceleration error in equations (3.1), (3.2), and (3.3), given by $\hat{V}^2/r_0$, ranges between approximately 0.1 and 1 ft/s^2. For many flight vehicles this is a negligible error. On the other hand, for a supersonic transport cruising eastward at 3000 ft/s this lowers the required steady-state lift by about 3 per cent, which could lower the drag significantly and hence make a noticeable difference in maximum range.

There appears to the authors to be no simple way to take these accelerations into account and still use a flight-path axis system referenced to the atmosphere. One could add an approximate correction acceleration in the vertical direction given by $\hat{V}^2/r_0$ to the translatory forces in equations (3.1), (3.2), and (3.3). In fact, one could further simplify the computation by adding the term only to equation (3.3), based on the argument that most of the time a supersonic aircraft will be in near-level flight at cruise and that a moderate acceleration error during transient conditions can be accepted.

In this case equation (3.3) becomes

$$-m\left(V_p Q_w - \frac{\hat{V}^2}{r_0}\right) = Z_w \qquad (3.15)$$

Note that this equation will exhibit acceleration errors of the order of $\hat{V}^2/r_0$ for conditions far from level flight.

4. ROTATIONAL EQUATIONS

The only reasonable axes to use for the rotational equations of motion are the body axes. If we let the external moment components along x_b, y_b, and z_b be L_b, M_b, and N_b, respectively, then summation of moments about the three body axes of a body symmetrical about the $x_b z_b$ plane leads to the equations:

$$I_{xx}\dot{P}_b - (I_{yy} - I_{zz})Q_bR_b - I_{xz}(\dot{R}_b + P_bQ_b) = L_b \qquad (4.1)$$

$$I_{yy}\dot{Q}_b - (I_{zz} - I_{xx})R_bP_b + I_{xz}(P_b^2 - R_b^2) = M_b \qquad (4.2)$$

$$I_{zz}\dot{R}_b - (I_{xx} - I_{yy})P_bQ_b - I_{xz}(\dot{P}_b - Q_bR_b) = N_b \qquad (4.3)$$

Here I_{xx}, I_{yy}, and I_{zz} are the moments of inertia about x_b, y_b, and z_b respectively, and I_{xz} is the product of inertia of the symmetrical body. Note in equations (4.1), (4.2), and (4.3) that the second term in each equation represents a nonlinear inertial coupling term. For flight vehicles such as large transport aircraft which do not generate relatively high angular rates these terms often can be neglected. For many flight vehicles the roll rate P_b has a maximum value which is considerably higher than pitch-rate Q_b or yaw-rate R_b. Hence the Q_bR_b term in equation (4.1) often can be neglected in comparison with the R_bP_b and P_bQ_b terms in equations (4.2) and (4.3), respectively.

The third term in each of equations (4.1), (4.2), and (4.3) represents the effect of the product of inertia I_{xz}. If the x, y, z body axes have been chosen to be almost coincident with the principal axes, this term may be negligible in all three equations, since I_{xz} will be very small compared with the principal moments of inertia. For relatively low angular rates the nonlinear terms (P_bQ_b, $P_b^2 - R_b^2$, and Q_bR_b) usually can be neglected and in any event R_b^2 frequently can be neglected as small compared with P_b^2 in equation (4.2).

5. COMPUTATION OF EULER ANGLES FOR A FLAT EARTH

Solution of equations (4.1), (4.2), and (4.3) results in computation of the body-axis angular velocity components P_b, Q_b, and R_b. These must be integrated a second time to obtain the orientation of the vehicle body axes with respect to the desired references axes, typically Euler axes which point north, east, and toward the center of the earth (x_e, y_e, and z_e in figure 5.1). This orientation usually is expressed in terms of the conventional aircraft Euler angles, *i.e.*, heading-angle ψ, pitch angle θ, and bank angle ϕ. These angles usually are computed from P_b, Q_b and R_b by the following well-known equations:

$$\dot{\psi} = (R_b \cos\phi + Q_b \sin\phi)/\cos\theta \qquad (5.1)$$

$$\dot{\theta} = Q_b \cos\phi - R_b \sin\phi \qquad (5.2)$$

$$\dot{\phi} = P_b + \dot{\psi} \sin\theta \qquad (5.3)$$

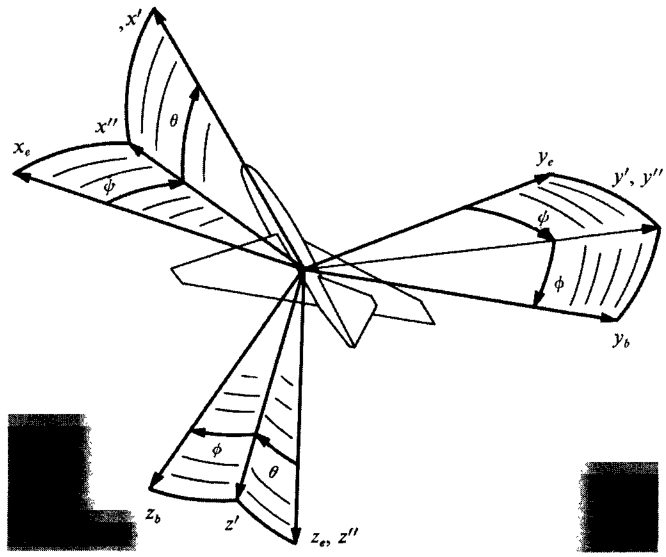

Figure 5.1 — Conventional aircraft Euler angles

Note that, since P_b, Q_b, R_b are the body-axis components of the vehicle angular velocity relative to an inertial reference system, there is a small error introduced by the angular velocity of axes which point north, east, and down relative to a spherical earth. This small error can be corrected, if necessary, using equations (7.1)–(7.3) in the next section.

The well known singularity of the Euler angle system at $\theta = \pm\pi/2$ can be avoided, if necessary, by computing direction cosines or quaternions[4] instead of Euler angles, or by introducing a fourth angle.[3]

The use of quaternions rather than direction cosines should be considered if a system free of singularities is needed, since there are only four quaternions with a single redundancy as compared with nine direction cosines with six redundancies.

6. COMPUTATION OF VEHICLE POSITION FOR A FLAT EARTH

Once the orientation of the flight vehicle with respect to the Euler axes has been established *e.g.*, by means of the Euler angles, then it is possible to compute the velocity north U_e, the velocity east V_e, and the velocity downward W_e, or its negative, the rate of climb $\dot{h}$. Direct integration then yields the vehicle position.

Determination of U_e, V_e, W_e is complicated by the fact that the vehicle velocity vector V_p lies along the x wind axis and therefore must be resolved from wind to earth axes. Unfortunately, the complete orientation of the wind axes is known only relative to body axes; hence it is necessary to perform the resolution of $\overline{V}_p$ into earth axes by first resolving it into body axes, then from body axes to earth axes. The resolution of $\overline{V}_r$ from wind axes to body axes is accomplished by the transformation given in equations (3.9), (3.10), and (3.11).

The resolution of vehicle velocity from body axes to earth axes can be accomplished by using direction cosines. Thus let l_1, l_2, and l_3 be the projections of a unit vector along the x body axis onto the x_e, y_e, and z_e earth axes, respectively. Similarly, let m_1, m_2, and m_3 be the projections of a unit vector along the y body axis onto the x_e, y_e, and z_e earth axes, respectively. In the same way let n_1, n_2, and n_3 be the projections of a unit vector the z body axis along the x_e, y_e, and z_e earth axes, respectively. Then by definition

$$\text{velocity north} = U_e = l_1 U_b + m_1 V_b + n_1 W_b \qquad (6.1)$$

$$\text{velocity east} = V_e = l_2 U_b + m_2 V_b + n_2 W_b \qquad (6.2)$$

$$\begin{aligned}\text{velocity downward} &= W_e = -\dot{h} \\ &= l_3 U_b + m_3 V_b + n_3 W_b \end{aligned} \qquad (6.3)$$

It is easy to show that the direction cosines are related to Euler angles by the following formulas:

$$\begin{aligned} l_1 &= \cos\theta\cos\psi \\ l_2 &= \cos\theta\sin\psi \\ l_3 &= -\sin\theta \end{aligned} \qquad (6.4)$$

$$\begin{aligned} m_1 &= -\cos\phi\sin\psi + \sin\phi\sin\theta\cos\psi \\ m_2 &= \cos\phi\cos\psi + \sin\phi\sin\theta\sin\psi \\ m_3 &= \sin\phi\cos\theta \end{aligned} \qquad (6.5)$$

$$\begin{aligned} n_1 &= \sin\phi\sin\psi + \cos\phi\sin\theta\cos\psi \\ n_2 &= -\sin\phi\cos\psi + \cos\phi\sin\theta\sin\psi \\ n_3 &= \cos\theta\cos\phi \end{aligned} \qquad (6.6)$$

(Equivalent formulas for direction cosines in terms of quaternions are given in reference 4.) An alternative mechanization of equations (6.1) through (6.6) avoids computation of the direction cosines by instead performing successive resolutions of the velocity components U_b, V_b, and W_b through the angles $-\phi$, $-\theta$, and $-\psi$. Consider the intermediate axis system x', y', z' in figure 5.1. Clearly the velocity components U', V', and W' along x', y', and z' are given by

$$\begin{aligned} U' = U_b, \qquad V' &= V_b\cos\phi - W_b\sin\phi \\ W' &= V_b\sin\phi + W_b\cos\phi \end{aligned} \qquad (6.7)$$

Defining U'', V'', and W'' as the velocity components along the intermediate axes x'', y'', and z'', we have

$$\begin{aligned} U'' = U'\cos\theta + W'\sin\theta, \qquad V'' &= V' \\ W'' &= -U'\sin\theta + W'\cos\theta \end{aligned} \qquad (6.8)$$

Finally, from figure 4.1 we see that

$$\begin{aligned} U_e &= U''\cos\psi - V''\sin\psi \\ V_e &= U''\sin\psi + V''\cos\psi \\ W_e &= -\dot{h} = W'' \end{aligned} \qquad (6.9)$$

Successive application of equations (6.7), (6.8), and (6.9) for U, V, and W to obtain U_e, V_e, and W_e requires fewer mathematical operations than using equations (6.1) through (6.6). It therefore has computational advantages using either an analog or digital mechanization. In computing ground coordinates from U_e and V_e in equations (6.1) and (6.2), or equation (6.9), it is important to note that U_e and V_e represent airspeed components north and east, respectively. To convert them to groundspeed components, the north component of wind w_x must be subtracted from U_e, and the east component of wind w_y must be subtracted from V_e. Thus if s_x and s_y represent distance traveled north and east, respectively, then

$$\dot{s}_x = U_e - w_x \qquad (6.10)$$

$$\dot{s}_y = V_e - w_y \qquad (6.11)$$

Equations (6.10) and (6.11) are valid only for steady winds, since the implicit assumption was made that axes stationary relative to the atmosphere are inertial. Equations (3.1), (3.2), and (3.3) are referred to inertial space and correction terms must be added if the reference axes are not inertial.

7. COMPUTATION OF VEHICLE EULER ANGLES AND POSITION FOR A ROTATING SPHERICAL EARTH

In the previous section we presented the formulas for computing vehicle position over a flat earth with steady winds. We can use the same position formulas to obtain velocity north U_e and velocity east V_e over a rotating spherical earth with radius r_0 and angular rate ω_N. However, U_e and V_e will represent airspeed components and must be corrected to yield groundspeed components $\dot{s}_x$ and $\dot{s}_y$, respectively. Furthermore, when a spherical earth is considered, it may be necessary to correct the vehicle angular rates used to compute Euler angles in order to take into account the rotating reference frame, as pointed out earlier in section 6. It can be shown that the body-axis components of the vehicle angular velocity relative to the Euler reference frame, P_{be}, Q_{be}, R_{be} are given by the following formulas:[5]

$$P_{be} = P_b - \frac{\dot{s}_y}{r} l_1 + \frac{\dot{s}_x}{r} l_2 + \frac{\dot{s}_y}{r} \tan L l_3 \quad (7.1)$$

$$Q_{be} = Q_b - \frac{\dot{s}_y}{r} m_1 + \frac{\dot{s}_x}{r} m_2 + \frac{\dot{s}_y}{r} \tan L m_3 \quad (7.2)$$

$$R_{be} = R_b - \frac{\dot{s}_y}{r} n_1 + \frac{\dot{s}_x}{r} n_2 + \frac{\dot{s}_y}{r} \tan L n_3 \quad (7.3)$$

Here r is the radial distance of the vehicle from the center of the earth and is given by

$$r = r_0 + h \quad (7.4)$$

where r_0 is the radius of the earth and h is the vehicle altitude. In many cases we can substitute r_0 for r in equations (7.1), (7.2), and (7.3) and still obtain sufficient accuracy.

The values of P_{be}, Q_{be}, and R_{be} in these equations are then used to compute the Euler angle rates. Thus by analogy with equations (5.1), (5.2), and (5.4)

$$\dot{\psi} = (R_{be} \cos\phi + Q_{be} \sin\phi)/\cos\theta \quad (7.5)$$

$$\dot{\theta} = Q_{be} \cos\phi - R_{be} \sin\phi \quad (7.6)$$

$$\dot{\phi} = P_{be} + \dot{\psi} \sin\theta \quad (7.7)$$

In many cases the computations involved in equations (7.1), (7.2), and (7.3) can be neglected *i.e.*, we can assume that $P_{be} \cong P_b$, $Q_{be} \cong Q_b$, $R_{be} \cong R_b$. This is particularly true if the overall six-degree-of-freedom computation involves a control system (automatic or human) which attempts to maintain ψ, θ, and ϕ at specified values. In any case the correction rates are the order of V_p/r_0. For example, if $V_p = 2000$ ft/s, the correction rate is equal to approximately 0.005 degree per second. On the other hand, if the flight-vehicle problem includes a stable platform, the rate corrections given by equations (7.1), (7.2), and (7.3) may be important.

It should be noted that $\dot{s}_x$ and $\dot{s}_y$ in equations (7.1), (7.2), and (7.3) represent vehicle velocity components north and east, respectively, over the surface of a nonrotating earth with steady winds. On the other hand equations (6.1) and (6.2), or alternatively, equation (6.9), gives us U_e and V_e, *i.e.*, vehicle velocity components north and east, respectively, relative to the inertial reference frame for the translational equations of motion. We made the approximation in section 3 that this reference frame is fixed relative to the ambient atmosphere. We can account for the linear velocity of the atmospheric reference frame (but not the angular velocity) by noting that relative to the surface of a nonrotating earth it is moving northward with the northerly component of wind and eastward with the sum of the rate due to earth spin and that due to eastward component of wind. Thus we can write the following equations:

$$\dot{s}_x = U_e - w_x \quad (7.8)$$

$$\dot{s}_y = V_e + \omega_N r \cos L - w_y \quad (7.9)$$

It can also be shown[5] that the time rate of change of latitude and longitude are given by the following formulas:

$$\dot{L} = \frac{\dot{s}_x}{r} \quad (7.10)$$

$$\dot{\lambda} = \frac{\dot{s}_y}{r \cos L} - \omega_N \quad (7.11)$$

It should be noted that motion of a flight-vehicle over a rotating earth can be treated exactly,[5] but that the exact translational equations referred to axes fixed relative to the ambient atmosphere are very complicated. Thus many of the computer mechanization advantages for flight-path axes are lost, and the computation of α, β, and V_p is much less elegant. We have attempted in this section to describe how one can utilize the flight-path axis system and still correct approximately for the fact that the vehicle is flying over a rotating earth with surface winds. This approach should be adequate for all but the most exacting requirements, unless the vehicle reaches hypersonic speeds. For subsonic vehicles or supersonic vehicles traveling over relatively short distances the flat-earth equations in sections 3 through 6 should be adequate.

8. COMPUTATION OF AERODYNAMIC FORCES AND MOMENTS

Aerodynamic forces and moments for flight vehicles normally are computed in stability axes. Thus let X_a, Y_a, and Z_a be the aerodynamic forces along the x_s, y_s, and z_s stability axes shown in figure 3.1. Here $-X_a$ corresponds to drag D, and $-Z_a$ corresponds to lift L.

In addition to aerodynamic forces the flight vehicle experiences propulsion and gravity forces. These are most conveniently defined in body axes. Let us denote the propulsion force components along the x and z body axes by X_p and Z_p, respectively. The gravity force components along x, y, and z will by definition be mgl_3, mgm_3, and mgn_3 respectively. The sum of the propulsive forces and gravity forces along body axes can then be resolved to stability axes, where the aerodynamic forces are added to obtain the total force component X_s, Y_s, and Z_s along the stability axes. Using equations (6.4), (6.5), and (6.6) to express the direction cosines l_3, m_3, n_3 in terms of Euler angles, we obtain:

$$X_s = (X_p - mg\sin\theta)\cos\alpha + (Z_p + mg\cos\theta\cos\phi)\sin\alpha - D \quad (8.1)$$

$$Y_s = mg\cos\theta\sin\phi + Y_a \quad (8.2)$$

$$Z_s = -(X_p - mg\sin\theta)\sin\alpha + (Z_p + mg\cos\theta\cos\phi)\cos\alpha - L \quad (8.3)$$

Finally, reference to figure 3.1 shows that the force components X_w, Y_w, and Z_w along the flight-path axes can be computed using the following formulas:

$$X_w = X_s\cos\beta + Y_s\sin\beta \quad (8.4)$$

$$Y_w = -X_s\sin\beta + Y_s\cos\beta \quad (8.5)$$

$$Z_w = Z_s \quad (8.6)$$

These force components are used to mechanize the translational equations given in section 3. If the aerodynamic forces are given in body axes rather than stability axes, the modification of equations (8.1), (8.2), and (8.3) is apparent.

The external moments acting on the flight vehicle consist of aerodynamic moments L_a, M_a, and N_a, normally given in stability axes, and power plant moments L_p, M_p, and N_p, given in body axes. The total moments L, M, and N in body axes become the following:

$$L_b = L_a\cos\alpha - N_a\sin\alpha + L_p \quad (8.7)$$

$$M_b = M_a + M_p \quad (8.8)$$

$$N_b = L_a\sin\alpha + N_a\cos\alpha + N_p \quad (8.9)$$

Again, if the aerodynamic moments are given in body axes, the simplification of equations (8.7), (8.8), and (8.9) is obvious (set $\alpha = 0$).

Figure 8.1 shows a block diagram of the over-all six-degree-of-freedom equations for the case of a flat earth.

REFERENCES

1 HOWE R M
Coordinate systems for solving the three-dimensional flight equations
WADC Technical Note 55-747 June 1956

2 HOWE R M
Coordinate systems and methods of coordinate transformation for three-dimensional flight equations
Proceedings of the First Flight Simulation Symposium WSPG Special Report 9 September 1957

3 GREENWOOD D T
An extended Euler angle coordinate system for use with all-altitude aircraft simulators
WADC Technical Report 60-372 August 1960

4 ROBINSON A C
On the use of quaternions in simulation of rigid-body motion
WADC Technical Report 58-17 December 1958

5 FOGARTY L E HOWE R M
Analog computer solution of the orbital flight equations
SIMULATION vol 1 no 1 Fall 1963 pp R-41 through R-47

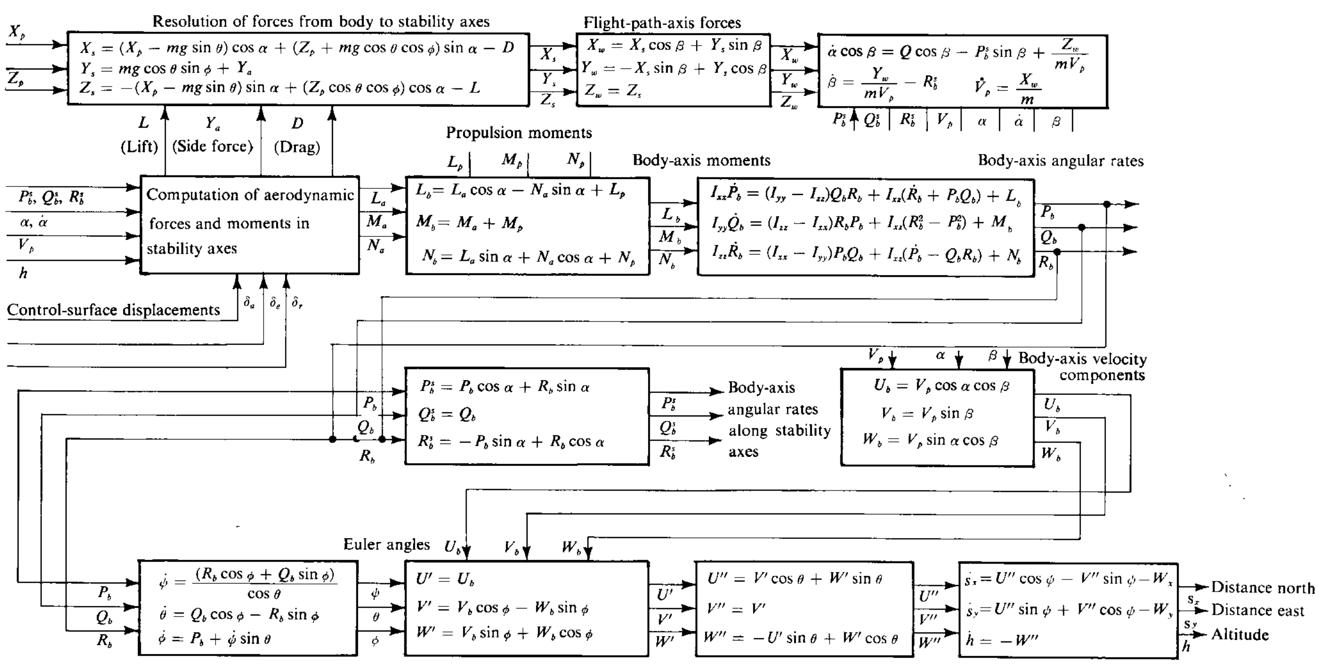

Figure 8.1—Block diagram of combined flight-path axis, body- axis system for a flat earth, steady winds